Pergamon

Bioorganic & Medicinal Chemistry 6 (1998) 1103–1115

BIOORGANIC & MEDICINAL CHEMISTRY

Structure–Cytotoxic Activity Relationship for the Toad Poison Bufadienolides

Yoshiaki Kamano,[a,*] Ayano Kotake,[a] Hirofumi Hashima,[a] Masuo Inoue,[a] Hiroshi Morita,[b] Koichi Takeya,[b] Hideji Itokawa,[b] Nobuyo Nandachi,[c] Toshiaki Segawa,[d] Ayako Yukita,[d] Kyoko Saitou,[e] Mariko Katsuyama[e] and George R. Pettit[f]

[a]*Faculty of Science, Kanagawa University, 2946 Tsuchiya, Hiratsuka, Kanagawa 259-12, Japan*
[b]*School of Pharmacy, Tokyo University of Pharmacy & Life Science, 1432-1 Horinouchi, Hachioji, Tokyo 192-03, Japan*
[c]*Ohme Institute, Tobishi Pharmaceutical Co. Ltd., 1-7-1 Suehiro, Ohme, Tokyo 198, Japan*
[d]*Tsukuba Institute, Toagousei Chemical Industry Co., 2 Ohkubo, Tsukuba, Ibaragi 300-33, Japan*
[e]*Sumisho Electronics Co., Ltd., 2-23 Shimomiyabi-cho, Shinjuku-ku, Tokyo 162, Japan*
[f]*Cancer Research Institute and Department of Chemistry, Arizona State University, Tempe, AZ 85287-1604, USA*

Received 13 February 1998; accepted 6 April 1998

Abstract—The toad poison bufadienolides including natural and derivatized compounds were tested for their cytotoxic effects on primary liver carcinoma cells PLC/PRF/5 and their structure–cytotoxic activity relationships were studied. For this study, a ligand-binding model was developed by using a pharmacophore mapping program, Distance Comparisons (DISCO). The structural features that are common to the 3D structures of active bufadienolides were identified to provide approach to a 3D QSAR method by using Comparative Molecular Field Analysis (CoMFA) study and to correlate the steric and electrostatic fields of the molecules to their activities. A valuable model which enables prediction of their activities was obtained from the CoMFA analysis, which may be employed for the drug designs of new bufadienolide analogues.

Introduction

The Chinese drug Ch'an Su, called 'Senso' in Japanese, is a product of the skin gland of toads such as *Bufo bufo gargarizans* etc., which has been used traditionally as a cardiotonic, diuretic, anodyne and hemostatic agent. Its major effective components, generally called, the toad poison or bufadienolides, have a novel steroidal A/B *cis* and C/D *cis* structure with an α-pyrone ring at C17-position and exhibit a range of biological activities, such as cardiotic, blood pressure stimulating, respiration, and antineoplastic activities. Of the bufadienolides, resibufogenin is now used as a cardiotonic drug, and bufalin has recently been reported to have a strong surface anesthetic activity[1] and cytotoxic effect and differentiation-apoptosis activity on murine leukemia HL-60 cells.[2]

In the present studies, cytotoxic activities of 80 bufadienolides, including derivatives and isomers of naturally occurring bufadienolides were studied on the cell line, primary liver carcinoma PLC/PRF/5. Of them, 16 were shown to have potent cytotoxicities ($IC_{50} < 10^{-3}$) and their structure–activity relationships were revealed to show the necessary structural features for the activities.

The three dimensional (3D) quantitative structure–activity relationships (QSAR) of these active compounds were studied by computational methods, in which, first, calculation was made to find the possible pharmacophores for those 16 potently cytotoxic compounds by using the Distance Comparisons (DISCO) program.[3] On the basis of the proposed pharmacophore model, 3D QSAR analysis was conducted by using Comparative Molecular field (CoMFA) analysis.[4] A suitable model was developed, which might provide reliable information about the activity and be useful for

*Corresponding author.

0968-0896/98/$19.00
PII: S0968-0896(98)00067-4

drug designing of active bufadienolides. The cell growth inhibitory activities of the bufadienolides derived from the calculations and those of bioassay were compared to show good agreement of these two sets of data.

Materials and Methods

General details

For biological test, chromatography and reactions, commercial solvents of analytical grade were used after redistillation. All melting points were determined on a micro hot-stage apparatus (Reichert, Austria) and uncorrected. Ultra violet spectra were measured with a SHIMAZU, UV 2500PC spectrometer, optical rotations, with a HORIBA, High Sensitive Polarimeter with the $[\alpha]_D$ values given in 10^{-1} deg cm^2 g^{-1}. EI and FAB mass spectra were taken with a JEOL JMS-AX505H mass spectrometer and IR spectra on a Jasco, FT/IR-300 spectrophotometer. Preparative high-pressure liquid chromatography (HPLC) was performed with an Inertsil PREP-ODS column (20 mm i.d.×250 mm, GL Science Inc.) packed with 10 μm ODS. TLC was conducted on precoated Kieselgel 60 F_{254} (Art. 5715; Merck) and the spots were detected by spraying with 5% sulfuric acid–ethanol solution and heating (hot plate). ^{1}H and ^{13}C NMR spectra were recorded on a JEOL 400EX spectrometer at 303 K. The NMR coupling constants (J) are given in Hz.

Materials

Ch'an Su, bufadienolides and cardenolides: Ch'an Su was obtained in Hong Kong folk-medical market. Of the 80 compounds tested, some were isolated from Ch'an Su, some were commercially obtained and some were derivatized from known bufadienolides in our laboratory.

Bufalin 3-succinate (**4**), bufalin 3-methacrylate (**5**), bufalin 3-[*N*-(*tert*-butoxycarbonyl)hydrazido] succinate (**8**),[9] 14β, 15β-epoxy-3-oxo-bufa-1, 20, 22-trienolide (Δ^1-3-oxo-resibufogenin) (**27**), 14β, 15β-epoxy-3-oxo-bufa-1, 4, 20, 22-tetraenolide ($\Delta^{1,4}$-3-oxo-resibufogenin) (**28**), desacetyl-cinobufagin 3-acetate-16-succinate (**48**), 3-oxo-14α-artebufogenin (**56**), digitoxigenin 3-methylsuberate (**67**), methyl 3β-hydroxy-14β, 15β; 16β, 22β-diepoxy-21-nor-5β, 14β-cholanoate (CMKA) (**76**), and methyl(*E*)-3β, 16β-dihydroxy-14β, 15β-epoxy-21-norchol-20(22)-enoate (CMKB) (**77**) were newly prepared from the corresponding starting materials as described below.

Bufalin 3-succinate (4). A mixture of bufalin (**1**: 15 mg) and succinic anhydride (30 mg) in pyridine (5 mL) was refluxed for 2 h and then poured into ice-water. It was extracted with $CHCl_3$. After removal of the solvent, the residue (16 mg) was chromatographed on a silica gel column. Elution with *n*-hexane-acetone (3:1) and recrystallization from acetone gave 9.5 mg of **4**, as a colorless prism, mp 227–229 °C, $[\alpha]_D$ −9.9° (*c* 0.5, $CHCl_3$), *m/z* 486(M)$^+$; λmax(MeOH)/nm 295 (log ε 3.20); ν_{max}(KBr)/cm^{-1} 3380–3110, 3038, 1742, 1729, 1718, 1675, 1620, 1545, 1265, 1245, 955, 800, 750; ^{1}H NMR ($CDCl_3$) δ 0.70 (3H, s, 18-CH_3), 0.95 (3H, s, 19-CH_3), 2.47 (1H, m, 17-H), 2.66 (4H, m, 2×CH_2 of succinate), 5.13 (1H, bs, 3-H), 6.28 (1H, d, J=9.8, 23-H), 7.24 (1H, d, J=1.5, 21-H), 7.84 (1H, dd, J=9.8, 2.4, 22-H); ^{13}C NMR ($CDCl_3$) δ 16.8 (C-18), 21.3 (C-19), 51.2 (C-17), 71.0 (C-3), 85.4 (C-14), 115.3 (C-23), 122.7 (C-20), 146.8 (C-22), 148.6 (C-21), 162.5 (C-24), 171.6 (3-O*CO*-$(CH_2)_2$COOH), 176.9 (3-OCO$(CH_2)_2$*CO*OH); Anal. calcd for $C_{28}H_{38}O_7$: C, 69.11; H, 7.87. Found: C, 69.02; H, 7.95.

Bufalin 3-methacrylate (5). To a solution of bufalin (**1**) (10 mg) in pyridine (3 mL), methacryloyl chloride (0.2 mL) was added. The mixture was allowed to stand for 3 h at room temperature and poured into ice-water. The solid thus obtained was collected and washed with water. Recrystallization of the crude product from MeOH gave 8.5 mg of 3-methacrylate (**5**), as a colorless needles: $[\alpha]_D$ −5.1° (*c* 1.0, $CHCl_3$); *m/z* 454(M)$^+$; λmax (CH_3CN)/nm 300 (log ε 3.33); ν_{max}(KBr)/cm^{-1} 3509, 2929, 2359, 1714, 1453, 1260, 1024, 798; ^{1}H NMR ($CDCl_3$) δ 0.71 (3H, s, 18-CH_3), 0.97 (3H, s, 19-CH_3), 1.96 (3H, s, 3-OCO (CH_3)C=CH_2), 2.49 (1H, m, 17-H), 5.16 (1H, bs, 3-H), 5.55 and 6.10 (2H, 3-OCO (CH_3)C=CH_2), 6.27 (1H, d, J=9.8, 23-H), 7.23 (1H, d, J=1.5, 21-H), 7.83 (1H, dd, J=9.8, 2.9, 22-H); ^{13}C NMR ($CDCl_3$): δ 16.5 (C-18), 21.4 (C-19), 30.5 (3-OCO (CH_3)C=CH_2), 51.3 (C-17), 70.5 (C-3), 85.4 (C-14), 115.4 (C-23), 122.6 (C-20), 125.0 (3-OCO(CH_3)C=CH_2), 137.1 (3-OCO(CH_3)*C*=CH_2), 146.7 (C-22), 148.6 (C-21), 162.5 (C-24), 166.8 (3-O*CO*-(CH_3)C=CH_2); Anal. calcd for $C_{28}H_{38}O_5$: C, 73.98; H, 8.43. Found: C, 73.77; H, 8.41.

Bufalin 3-[*N*-(*tert*-butoxycarbonyl)hydrazido]succinate (8). To a cold solution of bufalin 3-hemi-succinate (38 mg) and *tert*-butylcarbazoate (14 mg) in CH_2Cl_2 (2.8 mL) in ice bath was added triethylamine (0.01 mL) and 1-ethyl-3-[3α-(dimethylamino)propyl] carbodiimide hydrochlorine (EDCI) (15 mg) and the mixture was stirred for 5.5 h. Another 15 mg portion of EDCI was added to accelerate the formation of butoxycarbonyl hydrazide (**8**). Stirring was continued for another 2 h in ice-bath and for a day at room temperature. The mixture was then diluted with CH_2Cl_2 (5 mL) and poured into water. The CH_2Cl_2 layer was washed successively with water, 2% Na_2CO_3 and water. Evaporation of the solvent gave a slightly yellowish oily residue (55 mg). Silica gel column chromatography of the residue with *n*-hexane-acetone (3:1) gave 12 mg of pure butoxycarbonyl

hydrazide (**8**) as a colorless prism, mp 255–258 °C, $[\alpha]_D$ −8.3° (*c* 1.0, $CHCl_3$); *m/z* 600$(M)^+$; λmax(MeOH)/nm 297 (log ε 3.40); ν_{max}(KBr)/cm^{-1} 3600, 3355, 1740, 1678, 1655, 1552, 1240, 970, 835, 797; ^{1}H NMR ($CDCl_3$) δ 0.70 (3H, s, 18-CH_3), 0.95 (3H, s, 19-CH_3), 2.17 (1H, m, 17-H), 1.46 (9H, s, COOC(CH_3)$_3$), 2.53 and 2.70 (4H, each m, OCO(CH_2)$_2$CO), 5.10 (1H, bs, 3-H), 6.27 (1H, d, *J* = 9.8, 23-H), 6.59 (1H, bs, 3-OCO(CH_2)$_2$CO*NH*NH-COOC(CH_3)$_3$), 7.23 (1H, d, *J* = 1.5, 21-H), 7.76 (1H, bs, 3-OCO(CH_2)$_2$CONH*NH*COOC(CH_3)$_3$), 7.84 (1H, dd, *J* = 9.8, 2.9, 22-H); ^{13}C NMR($CDCl_3$) δ 16.6 (C-18), 21.3 (C-19), 28.1 (COOC(CH_3)$_3$), 53.8 (C-17), 71.1 (C-3), 81.9 (COO*C*(CH_3)$_3$), 85.4 (C-14), 115.3 (C-23), 122.7 (C-20), 146.8 (C-22), 148.6 (C-21), 155.4 (3-OCO(CH_2)$_2$*CO*NHNHCOOC(CH_3)$_3$), 162.5 (C-24), 171.4 (3-O*CO*(CH_2)$_2$CONHNHCOOC(CH_3)$_3$), 172.3 (3-OCO(CH_2)$_2$CONHNH*CO*OC(CH_3)$_3$); Anal. calcd for $C_{33}H_{48}N_2O_8$: C, 65.97; H, 8.05; N, 4.66. Found: C, 66.03, H, 7.92, N, 4.63.

14b,15β-Epoxy-3-oxo-bufa-1,20,22-trienolide(Δ^1-3-oxo-resibufogenin) (27) and 14β, 15β-epoxy-3-oxo-bufa-1,4,20,22-tetraenolide($\Delta^{1,4}$-3-oxo-resibufogenin) (28). A mixture of 3-oxo-resibufogenin (**26**)[12] (1.25 g, 3.27 mmol) and 2,3-dichloro-5,6-dicyano-1,4-benzoquinone(DDQ) (816 mg, 3.6 mmol) in dioxane (30 mL) was refluxed for 4 h. The reaction mixture was mixed with silica gel (10 g), which was dried and placed on a silica gel column (700×30 mm). The column was eluted with *n*-hexane-acetone (4:1) to give four major fractions. **27** was isolated from the second fraction, which was further purified by preparative TLC. Compound **27**: colorless needles, mp 221–223 °C, $[\alpha]_D$ +70° (*c* 0.83, $CHCl_3$); *m/z* 380 $(M)^+$; λmax(MeOH)/nm 297 (log ε 2.42), 223 (log ε 2.99); ν_{max}(KBr)/cm^{-1} 2963, 2936, 2872, 1742, 1723, 1696, 1680, 1538, 1124, 952, 825, 830, 785; ^{1}H NMR($CDCl_3$) δ 0.75 (3H, s, 18-CH_3), 1.16 (3H, s, 19-CH_3), 2.45 (1H, m, 17-H), 3.46 (1H, s, 15-H), 5.94(1H, d, *J* = 10.2, 2-H), 6.18 (1H, dd, *J* = 9.7, 0.9, 23-H), 6.78 (1H, d, *J* = 10.2, 1-H), 7.17 (1H, dd, *J* = 2.7, 0.9, 21-H), 7.70 (1H, dd , *J* = 9.7, 2.8, 22-H); ^{13}C NMR ($CDCl_3$) δ 16.8 (C-18), 20.7 (C-19), 59.8 (C-17), 73.8 (C-15), 115.4 (C-23), 122.0 (C-20), 127.7 (C-1, C-2), 146.8 (C-22), 149.7 (C-21), 160.1 (C-24), 200.1 (C-3); Anal. calcd for $C_{24}H_{28}O_4$: C,75.76; H, 7.42. Found: C, 75.98; H, 7.35.

The fourth fraction was dried and the residue was recrystallized from acetone-hexane to give 170 mg (14%) of tetraenolide (**28**) as a colorless needles, $[\alpha]_D$ +20.0° (*c* 1.0, $CHCl_3$); *m/z* 378 $(M)^+$; λmax(MeOH)/nm 298 (log ε 3.73), 236 (log ε 4.19); ν_{max}(KBr)/$cm^{\xi 1}$ 2940, 2871, 1746, 1722, 1662, 1642, 1538, 1124, 950, 832, 785; ^{1}H NMR($CDCl_3$) δ 0.86 (3H, s, 18-CH_3), 1.26 (3H, s, 19-CH_3), 2.17 (1H, m, 17-H), 3.46 (1H, s, 15-H), 6.35 to 6.0 (3H, m, 23-H, 2-H, 4-H), 7.05 (1H, d, *J* = 10.0, 1-H), 7.25 (1H, dd, *J* = 1.6, 0.9, 21-H), 7.75 (1H, dd, *J* = 9.9, 1.6, 22-H); ^{13}C NMR($CDCl_3$) δ 16.8 (C-18), 18.8 (C-19), 59.7 (C-17), 73.6 (C-15), 115.4 (C-23), 121.8 (C-20), 124.3 (C-1), 128.0 (C-2), 146.7 (C-22), 149.7 (C-21), 154.4 (C-4), 161.9 (C-24), 167.6 (C-5), 186.0 (C-3); Anal. calcd. for $C_{24}H_{26}O_4$: C,76.16; H, 6.93. Found: C, 75.89; H, 7.07.

Desacetyl-cinobufagin 3-acetate-16-succinate (48). A mixture of **47** (500 mg),[1] succinic anhydride (500 mg) and pyridine (10 mL) was refluxed for 4 h. The mixture was poured into ice-water and extracted with $CHCl_3$. After the removal of solvent, the residue (553 mg) was chromatographed on a silica gel column with *n*-hexane-acetone (3:1). Recrystallization from *n*-hexane-acetone gave 495 mg of colorless needles of **48**: $[\alpha]_D$ +10.7° (*c* 1.0, $CHCl_3$); *m/z* 542$(M)^+$; λmax(MeCN)/nm 295 (log ε 3.38); ν_{max}(KBr)/cm^{-1} 3400–3100, 1740, 1720, 1700, 1645, 1545, 1250, 1235, 958, 894, 790; ^{1}H NMR ($CDCl_3$) δ 0.83 (3H, s, 18-CH_3), 1.00 (3H, s, 19-CH_3), 2.07 (3H, s, 3-OCO*CH*$_3$), 2.55 (4H, m, 2×CH_2 of succinate), 2.81 (1H, d, *J* = 9.5, 17-H), 3.68 (1H, d, *J* = 1.5, 15-H), 5.10 (1H, bs, 3-H), 5.53 (1H, dd, *J* = 9.5, 1.5, 16-H), 6.25 (1H, d, *J* = 10.2, 23-H), 7.19 (1H, d, *J* = 3.0, 21-H), 7.95 (1H. dd, *J* = 10.2, 3.0, 22-H); ^{13}C NMR ($CDCl_3$) δ 17.2 (C-18), 23.7 (C-19), 50.4 (C-17), 59.5 (C-15), 70.2 (C-3), 72.3 (C-14), 75.1 (C-16), 114.1 (C-23), 116.2 (C-20), 148.3 (C-22), 151.4 (C-21), 162.3 (C-24), 170.7 (3-O*CO*CH_3), 171.5 (16-O*CO*(CH_2)$_2$COOH), 175.5 (16-OCO(CH_2)$_2$*CO*OH); Anal. calcd for $C_{30}H_{38}O_9$: C,66.40; H, 7.06. Found: C, 66.44; H, 7.02.

3-Oxo-14α-artebufogenin (56). To a solution of 14α-artebufogenin (**55**)[15] (50 mg) in acetic acid (3 mL), a solution of chromic acid (10 mg) in acetic acid (1 mL) was added with stirring. The oxidation was conducted at 15–18 °C for 4 h. After decomposition of the excess reagent with MeOH (0.25 mL, with stirring), the mixture was poured into ice-water and extracted with $CHCl_3$. The extract was washed with water and concentrated to dryness. Recrystallization of the crude product from MeOH gave 37 mg of 3-oxo-14α-artebufogenin (**56**) as a colorless needles: mp 210–213 °C, $[\alpha]_D$ +47.6° (*c* 1.0, $CHCl_3$); *m/z* 382 $(M)^+$ for $C_{24}H_{30}O_4$; λmax(MeCN)/nm 298 (log ε 3.70); ν_{max}(KBr)/cm^{-1} 2933, 2855, 1742, 1639, 1541, 1450, 1386, 1322, 1249, 1227, 1204, 1123, 990, 950, 833, 789; ^{1}H NMR ($CDCl_3$) δ 0.67 (3H, s, 18-CH_3), 1.05 (3H, s, 19-CH_3), 1.82 (1H, m, 14-H), 2.79 (1H, m, 17-H), 6.34 (1H, d, *J* = 1.0, 23-H), 7.27 (1H, dd, *J* = 12.7, 2.9, 22-H), 7.33(1H, m, 21-H); ^{13}C NMR ($CDCl_3$) δ 13.9 (C-18), 20.3 (C-19), 64.8 (C-14), 115.8 (C-20), 116.1 (C-23), 144.1 (C-22), 149.1 (C-21), 161.4 (C-24), 212.4 (C-3), 212.5 (C-15). Anal. calcd for $C_{24}H_{30}O_4$: C,75.36; H, 7.91. Found: C, 75.57; H, 7.95.

Digitoxigenin 3-methylsuberate (67). To a solution of digitoxigenin 3-suberate (**66**) (100 mg) in Et_2O (10 mL), a solution of CH_2N_2 (ca. 6 mg) in Et_2O (15 mL) was

added and the mixture was allowed to stand at room temperature for 10 min. The solvent was evaporated carefully in vacuo and the residue was purified by silica gel column chromatography with *n*-hexane-acetone mixture to give 85 mg of **67** as colorless prisms: $[\alpha]_D$ +42.2° (*c* 1.0, $CHCl_3$); *m/z* 544 $(M)^+$ for $C_{32}H_{48}O_7$; λmax(MeCN)/nm 216 (log ε 4.22), 272 (log ε 3.01)nm; ν_{max}(KBr)/cm^{-1} 3550, 3098, 2941, 2877, 1782, 1749, 1718, 1619, 1446, 1380, 1255, 1213, 1170, 1154, 1065, 1024, 956, 925. 887; ^{1}H NMR ($CDCl_3$) δ 0.88 (3H, s, 18-CH_3), 0.96 (3H, s, 19-CH_3), 2.78 (1H, m, 17-H), 3.67 (3H, s, 3-OCO$(CH_2)_6$-COOCH_3), 4.81 and 4.99 (2H, dd, *J* = 18.1, 1.46, 21-H), 5.10 (1H, m, 3-H), 5.88 (1H, s, 22-H), ^{13}C NMR ($CDCl_3$) δ 15.8 (C-18), 23.7 (C-19), 28.8 (3-OCO$(CH_2)_6$-COOCH_3), 50.9 (C-17), 70.1 (C-3), 73.4 (C-21), 85.5 (C-14), 117.7 (C-22), 173.2 (C-23), 174.1 (3-O*CO*$(CH_2)_6$COOCH$_3$), 174.5 (C-20 and 3-OCO$(CH_2)_6$*CO*OCH$_3$). Anal. calcd for $C_{32}H_{48}O_7$: C,70.56; H, 8.88. Found: C, 70.48; H, 8.95.

Methyl 3β-hydroxy-14β,15β; 16β,22β-diepoxy-21-nor-5β,14β-cholanoate (CMKA) (76) and methyl(*E*)-3β,16β-dihydroxy-14β,15β-epoxy-21-nor-chol-20(22)-enoate (CMK B) (77). Cinobufagin (**36**) (1.0 g) was dissolved in 0.1 N KOH in MeOH (50 mL) and the mixture was allowed to stand for 6 h at room temperature. The reaction mixture was acidified to pH 3–5 by addition of 10% *p*-toluenesulfonic acid in MeOH–water (1:1). By evaporation, the volume was reduced to about one third. The mixture was poured into ice-water and extracted with $CHCl_3$. The $CHCl_3$ layer was washed with aqueous Na_2CO_3 and water and evaporated to dryness to give a residue (1.02 g) which was chromatographed on a silica gel column. Elution with *n*-hexane-acetone (7:1, 6:1, and 4:1) gave 313 mg of crude CMKA (**76**), and 142 mg of CMKB (**77**). Recrystallization of the crude CMKA from acetone gave 296 mg of needles of **76** and recrystallization of the crude CMKB (**77**) from n-hexane-acetone gave 281 mg of needles of 77. CMKA (**76**): colorless needles, $[\alpha]_D$ +25.0° (*c* 1.0, $CHCl_3$); *m/z* 404 $(M)^+$, 386 $(M\text{-}H_2O)^+$; ν_{max}(KBr)/cm^{-1} 3500, 3050, 1745, 1190, 1145, 1095, 1075, 1037, 1003, 937, 915, 757; ^{1}H NMR ($CDCl_3$) δ 0.98 (3H, s, 18-CH_3), 1.06 (3H, s, 19-CH_3), 1.80 and 1.67 (2H, m, H-20), 2.29 (1H, ddd, *J* = 11.5, 8.3, 3.2, 17-H), 2.57 and 2.74 (2H, d *J* = 6.0, 7.0, 22-CH_2), 3.40 (1H, bs, 15-H), 3.69 (3H, s, 24-OCH_3), 4.13 (1H, br m, 3-H), 4.27 (1H, m, 21-H), 4.55 (1H, dd, *J* = 8.0, 1.5, 16-H), ^{13}C NMR ($CDCl_3$) δ 15.4 (C-19), 20.5 (C-7), 20.6 (C-11), 23.8 (C-18), 25.7 (C-6), 27.8 (C-2), 29.5 (C-1), 33.3 (C-4), 33.4 (C-8), 35.5 (C-20), 35.5 (C-10), 36.5(C-5), 39.2 (C-9), 39.5 (C-12), 40.3 (C-22), 41.3 (C-13), 51.6 (C-24-OCH3), 52.7 (C-17), 60.3 (C-15), 66.8 (C-3), 77.0 (C-14), 78.1 (C-21), 82.1 (C-16),172.0 (C-23); Anal. Calcd for $C_{24}H_{36}O_5$: C, 71.25; H, 8.97. Found: C, 71.26; H, 9.02. CMKB (**77**): colorless needles, $[\alpha]_D$ −5.7° (*c* 1.0, $CHCl_3$); *m/z* 432 $(M)^+$, 414$(M\text{-}H_2O)^+$, 404$(M\text{-}CO)^+$, 386 $(M\text{-}CO\text{-}H_2O)^+$; ν_{max}(KBr)/cm^{-1} 3560, 3500–3400, 3050, 2720, 1730, 1300, 1226, 1095, 1030, 978, 768; ^{1}H NMR ($CDCl_3$) δ 0.98 (3H, s, 18-CH_3), 1.05 (3H, s, 19-CH_3), 2.64 (1H, dd, *J* = 10.8, 8.4, 17-H), 2.84 (2H, dd, *J* = 16.1, 7.3, 22-CH_2), 3.04 (1H, ddd, *J* = 9.9, 9.5, 3.3, 20-H), 3.41 (1H, bs, 15-H), 3.69 (3H, s, 24-OCH_3), 4.13 (1H, br m, 3-H), 4.45 (1H, ddd, *J* = 9.2, 7.3, 5.5, 21-H), 4.72 (1H, dd, *J* = 8.4 , 1.1, 16-H), 9.58(1H, d, *J* = 3.3, 25-H). ^{13}C NMR ($CDCl_3$) δ 15.7 (C-19), 20.5 (C-11), 20.5 (C-7), 23.8 (C-18), 25.6 (C-6), 27.8 (C-2), 29.5 (C-1), 33.2 (C-8), 33.3 (C-4), 35.5 (C-10), 35.9 (C-5), 39.2 (C-9), 39.3 (C-12), 39.9 (C-22), 42.0 (C-13), 51.8 (C-24-OCH_3), 54.1 (C-17), 60.0 (C-15), 60.1 (C-20), 66.8 (C-3), 76.7 (C-14), 78.3 (C-21), 82.9 (C-16),171.2 (C-23), 200.7(C-25). Anal. calcd for $C_{25}H_{36}O_6$: C, 69.42; H,8.39. Found: C, 69.48; H, 8.41.

Bioassay

Primary liver carcinoma PLC/PRF/5 cells were maintained in tissue culture flasks and grown in 96-well microtiter plates for the assay. Appropriate dilutions of the test compounds (10^2–10^{-6} μg/mL) were added to the culture. After incubation at 37 °C, 5%CO_2, for 72 h, the survival rate of the cells in the cultures were evaluated by the MTT method. The effect was shown as IC_{50}, which is the concentration of test compound (μg/mL) to give 50% inhibition of the growth of PLC cells.

Computational methods

Sybyl molecular modeling software (version 6.3) was used for all molecular modeling techniques and CoMFA studies.[4] The compounds were built from fragments in the SYBYL database. Each structure was fully geometry-optimized by using the standard Tripos molecular mechanics force field with a distance-dependent dielectric function and a 0.01 kcal/mol energy-gradient convergence criterion. In addition, each stable conformer of side chains including δ-lactone ring at C-17 was obtained by using the systematic search routine in SYBYL. Partial atomic charges required for calculation of the electrostatic interaction energies were calculated by using the Gasteiger–Marsili method.[30]

Calculations of ring centroids, least square fitting, and excluded volume analyses were also carried out on 16 active bufadienolides ($IC_{50} < 10^{-3}$) by using DISCO program[3] in SYBYL. The pharmacophore mapping strategy was the calculation of the location of the ligand and site points, followed by execution of DISCO to find pharmacophore maps. Other compounds were aligned via this pharmacophore model.

For each of the alignment sets, the steric and Coulombic potential energy fields were separately calculated at each

lattice intersection on a regularly spaced grid of 2.0 Å units in all x, y, and z directions. The steric term represents the van der Waals interactions, whereas the Coulombic term represents the electrostatic interactions for which a distance-dependent dielectric expression $\varepsilon = R_{ij}$ was adopted. The grid pattern was generated automatically by the SYBYL/CoMFA routine. An sp^3 carbon atom with a +1.0 charge was selected as the probe for calculation of the steric and electrostatic field. Values of the steric and electrostatic energies were truncated at 30 kcal/mol.

To obtain a 3D-QSAR, partial least squares (PLS)[31] method was used. The PLS method was used successfully in many QSAR studies for rationalization of those structural features affecting the biological activity. The PLS algorithm was initially used with the cross-validation option to obtain the optimal number of components needed for the subsequent analysis of the data. In the leave-one-out cross-validation, each compound was systematically excluded from the set and its activity predicted by a model derived from the rest of the compounds. The optimal number of components was then chosen as that which yielded either the smallest rms error or the largest cross-validated r^2 value. A final PLS analysis was then performed by using the reported optimum number of components, with no cross-validation. This generated a fitted correlation of the entire training set with conventional r^2 values. The steric and electrostatic fields were scaled according to the CoMFA standard deviations in order to give the same potential weights on the resulting QSAR. The 3D-QSAR calibration model so derived was then employed to give theoretical inhibitory effect values of 10 bufadienolide derivatives which were compared with their bioassay data.

Results and Discussion

Cytotoxicity

The cytotoxic activities (IC_{50} μg/mL) of the 80 natural and derivatized bufadienolides and cardenolides on PLC cells are shown in Table 1. Of the natural bufadienolides, 20 (**1**, **6**, **9**, **13**, **14**, **15**, **18**, **19**, **21**, **23**, **35**, **36**, **40**, **46**, **50**, **51**, **53**, **55**, **63**, and **64**) were active on PLC cells (IC_{50} < 8.2 μg/mL). Hellebrigenin (**19**) having an aldehyde group at C-19, bufalin 3-acetate (**3**), gamabufotalin (**15**), and bufalin (**1**) were significantly active (IC_{50} 1.6–2.8 × 10^{-4} μg/mL). 14β-Hydroxy derivatives were generally more active than 14β, 15β-epoxy compounds and open α-pyrone ring compounds. Similar structure–activity relations have been reported on the surface anaesthic activities[1] and rhinovirus inhibitory activities[9] of bufadienolides.

Structure–activity relationships (SAR) consideration

Bufadienolides, cardenolides and their derivatives were divided into A–E groups, group A: 14-hydroxy compounds (**1**–**20**, **60**–**62**); group B: 14, 15-epoxy compounds (**21**–**51**); group C: cardenolides and their derivatives (**63**–**68**); group D: other bufadienolides (**52**–**59**), and group E: derivatives with cleaved α-pyrone ring (**69**–**80**). The structure and activity relationship revealed for each group may be summarized as follows.

Group A (1–20, 60–62)

To bufalin (**1**) having a basic structure, introduction of 19-aldehyde (**19**) or 11α-hydroxy (**15**) group indicated a tendency of the enhancive activity in 10^{-4} order, whereas that of 16β-acetoxy (**13**), 16β-hydroxy (**14**) or 5β-hydroxy (**18**) group indicated a tendency to reduce it. In addition to introduction of 15α-hydroxy (**60** and **61**) group, epimerization of 3β-hydroxy or 14β-hydroxy group to corresponding α-isomers (**2** and **10**) remarkablely reduced activity. On the other hand, introduction of a double bond to C-4 position (**11**) did not reduce the activity of bufalin (**1**). The activity of bufalin (**1**) was increased by acetylation of 3β-hydroxy group (**3**), but other 3-esterified derivatives (**4**–**8**) and 3-keto derivative (**9**) had lower activities than bufalin (**1**). It is interesting that the activity of 3-[*N*-(tert-butoxycarbonyl)hydrazide]-succinate (**8**) and 3-suberate (**6**) were stronger than that of 3-succinate (**4**).

Group B (21–51)

In this group, only cinobufagin (**36**) showed the strong activity of 10^{-4} order. Also, cinobufotalin (**50**) and resibufagin (**21**) kept their activity to 10^{-3} order. Thus, introduction of 19-aldehyde (**21**) group to resibufogenin (**23**) having a basic structure increased the activity, but that of 19-CH_2OH (**22**) group decreased it. For C-16 position, introduction of acetoxy group increased remarkabely the activity, as in the case of resibufogenin (**23**) and cinobufagin (16-acetoxy resibufogenin: **36**), or marinobufagin (**35**) and cinobufotalin (16-acetoxy marinobufagin: **50**), but that of hydroxy (**46**, **47**, **49** and **51**) or ester group (**48**) reduced it. Introduction of 5β-hydroxy (**35** and **50**) group reduced the activity. Also, introduction of an ester (**38**–**41**, **43**, and **47**) or oxo-group (**26**, **32**, **42**, and **44**) to C-3 position and that of double bond to C-1 and C-4 (**27** or **28**) decreased the activity. In generally, the activity of cinobufagin derivatives kept higher value than that of resibufogenin derivatives by reason of the effect of 16β-acetoxy group. Combination of various substituents at C-3 and C-16 may affect the potency of cytotoxicities on PLC cells. The sudden drop in activity appeared on epimerization of 3β-hydroxy (**30** and **36**) group and 14β, 15β-epoxy

(**25**, **26**, and **38**) group into corresponding 3α-hydroxy (**31** and **37**) and 14α, 15α-epoxy (**30**, **33** and **49**) group.

Group C (63–68)

The activities of cardenolides were generally weaker than those of corresponding bufadienolides having the same steroidal skeletons. Introduction of 5β-hydroxy (**63**) group or an ester function at C-3 (**65**–**67**) reduced the activity. It is interesting that the activity of 3-methylsuberate (**67**) was higher than that of 3-suberate (**66**).

Group D (52–59)

Miscellaneous bufadienolides and cardenolides, of which C-14 position did not carry any oxygen group, were collected. From that the compounds in this group

Table 1. The cytotoxicity of bufadienolides and related compounds against PLC/PRF/5 cell

No.	Compds	IC_{50}(μg/mL)
1	Bufalin[5]	2.8×10^{-4}
2	3α-Hydroxy-bufalin[6]	7.6×10^{-2}
3	Bufalin-3-acetate[7]	2.0×10^{-4}
4	Bufalin-3-succinate	6.6×10^{-2}
5	Bufalin-3-methacrylate	5.9×10^{-2}
6	Bufalin-3-suberate[8]	7.5×10^{-4}
7	Bufalin-3-methylsuberate[8]	9.0×10^{-3}
8	Bufalin-3-[*N*-(*tert*-butoxycarbonyl) hydrazido]succinate[9]	6.2×10^{-4}
9	3-oxo-Bufalin[10]	9.3×10^{-3}
10	14α-Hydroxy-bufalin-3β,16β-diacetate[7]	7.5
11	Scillarenin[10]	3.1×10^{-4}
12	3-oxo-Sillarenin[10,11]	1.9×10^{-4}
13	Bufotalin[5]	3.4×10^{-4}
14	Desacetyl-bufotalin[5]	7.8×10^{-4}
15	Gamabufotalin[5]	2.3×10^{-4}
16	Gamabufotalin-3-acetate[12]	6.0×10^{-2}
17	3-oxo-Gamabufotalin-11-acetate[12]	7.9×10^{-1}
18	Telocinobufagin[5]	3.5×10^{-4}
19	Hellebrigenin[5]	1.6×10^{-4}
20	Acetyl-arenobufagin[13a,13b]	8.7×10^{-1}
21	Resibufagin[14,15]	8.9×10^{-3}
22	Resibufaginol[14,15]	6.1×10^{-1}
23	Resibufogenin[5]	7.7×10^{-2}
24	3α-Hydroxy-resibufogenin[6]	8.3
25	Resibufogenin-3-acetate[16]	3.2×10^{-1}
26	3-oxo-Resibufogenin[6]	5.8
27	Δ^{1}-3-oxo-Resibufogenin	2.6
28	$\Delta^{1,4}$-3-oxo-Resibufogenin	6.7
29	16α-Hydroxy-resibufogenin-3-acetate[17]	6.7
30	14α,15α-Epoxy-resibufogenin[18]	20
31	3α-Hydroxy-14α,125α-epoxy-resibufogenin[6]	4.7
32	3-oxo-14α,15α-Epoxy-resibufogenin[6]	8.7
33	14α,15α-Epoxy-resibufogenin-3-acetate[18]	5.9
34	14α,15α-Epoxy-resibufogenin-3α-acetate[6]	4.7
35	Marinobufagin[5,14]	5.2×10^{-1}
36	Cinobufagin[5]	7.4×10^{-4}
37	3α-Hydroxy-cinobufagin[6]	9.8×10^{-2}
38	Cinobufagin-3-acetate[19]	4.0×10^{-2}
39	Cinobufagin-3-succinate[19]	8.5×10^{-1}
40	Cinobufagin-3-suberate[8]	1.0×10^{-2}
41	Cinobufagin-3-cinnamate[19]	6.4
42	3-oxo-Cinobufagin[20]	5.6×10^{-2}
43	Cinobufagin-3,5-dinitrobenzoate[19]	7.8×10^{-1}
44	3,16-Diketo-cinobufagin[19]	8.5×10^{-1}
45	16-oxo-Cinobufagin-3-acetate[17,19]	2.4
46	Desacetyl-cinobufagin[5]	5.2×10^{-1}
47	Desacetyl-cinobufagin-3-acetate[19]	9.8×10^{-2}
48	Desacetyl-cinofufagin-3-acetate-16-succinate	50
49	Desacetyl-14α,15α-epxoy-cinobufagin-3-acetate[17]	8.8×10^{-1}
50	Cinobufotalin[5]	1.0×10^{-3}
51	Desacetyl-cinobufotalin[5]	6.7×10^{-1}
52	β-Chlorohydrin[21]	7.0×10^{-2}
53	14β-Artebufogenin[5,16]	8.2×10^{-1}
54	14β-Artebufogenin-3-acetate[15]	5.5×10^{-1}
55	14α-Artebufogenin[5,15]	8.2
56	3-oxo-14α-Artebufogenin	7.0
57	Δ^{14}-Bufalin[18]	8.3×10^{-1}
58	Δ^{14}-3-oxo-Bufalin[18]	4.9
59	Δ^{14}-Bufotalin-3-acetate[23]	5.0
60	15α-Hydroxy-bufalin[22]	35
61	15α-Hydroxy-bufalin-3-acetate[23]	7.1×10^{-1}
62	15-oxo-Bufalin-3-acetate[24]	7.7×10^{-2}
63	Periplogenin[25]	6.1×10^{-2}
64	Digitoxigenin[5]	8.7×10^{-4}
65	Digitoxigenin-3-acetate[26]	5.5×10^{-1}
66	Digitoxigenin-3-suberate[19]	5.2
67	Digitoxigenin-3-methylsuberate	5.3×10^{-1}
68	Δ^{14}-Digitoxigenin[26]	3.6×10^{-1}
69	Isobufalin[27]	10
70	Isobufalin Me-ester[27]	9.1
71	Isobufalin Me-ester-3-acetate[27]	6.6
72	Isobufalin Et-ester[27]	7.5
73	Isobufalin Et-ester-3-acetate[27]	6.4
74	Isobufotalin Me-ester-3-acetate[27]	49
75	Isogamabufotalin Me-ester-3,11-diacetate[27]	9.7
76	CMKA	9.5
77	CMKB	26
78	RRA-1[28]	> 50
79	14β-arte-MK[29]	8.4
80	14β-arte-Et-K-Ac[29]	22

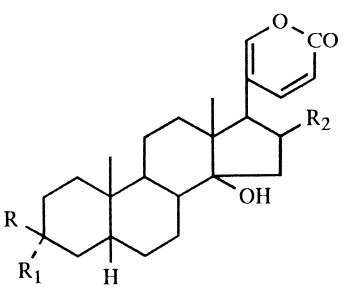

Group A

1 bufalin R=OH, R1=H, R2=H
2 3α-hydroxy-bufalin R=H, R1=OH, R2=H
3 bufalin-3-acetate R=OCOCH3, R1=H, R2=H
4 bufalin-3-succinate R=OCO(CH2)2COOH, R1=H, R2=H
5 bufalin-3-methacrylate R=OCOC(CH3)=CH2, R1=H, R2=H
6 bufalin-3-suberate R=OCO(CH2)6COOH, R1=H, R2=H
7 bufalin-3-methylsuberate R=OCO(CH2)6COOCH3, R1=H, R2=H
8 bufalin-3-[N-(tert.-butoxycarbonyl)hydrazido]succinate R=OCO(CH2)2CONHNHCOOC(CH3)3, R1=H, R2=H
9 3-oxo-bufalin R+R1=O, R2=H
10 14α-hydroxy-bufalin-3β,16β-diacetate R=OCOCH3, R1=H, R2=OCOCH3, 14-αOH
11 scillarenin R=OH, R1=H, R2=H, Δ4
12 3-oxo-sillarenin R+R1=O, R2=H, Δ4
13 bufotalin R=OH, R1=H, R2=OCOCH3
14 desacetyl-bufotalin R=OH, R1=H, R2=OH

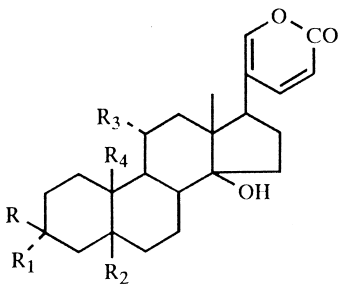

Group A

15 gamabufotalin R=OH, R1=H, R2=H, R3=OH, R4=CH3
16 gamabufotalin-3-acetate R=OCOCH3, R1=H, R2=H, R3=OH, R4=CH3
17 3-oxo-gamabufotalin-11-acetate R+R1=O, R2=H, R3=OCOCH3, R3=CH3
18 telocinobufagin R=OH, R1=H, R2=H, R3=H, R4=CH3
19 hellebrigenin R=OH, R1=H, R2=OH, R3=H, R4=CHO
20 acetyl-arenobufagin R=OCOCH3, R1=H, R2=H, R3=OH, R4=CH3, 12-ketone

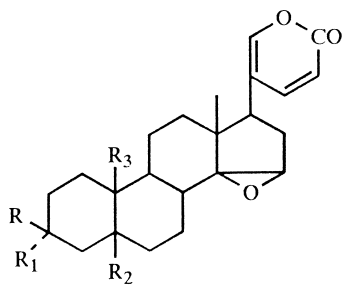

Group B

21 resibufagin R=OH, R1=H, R2=H, R3=CHO
22 resibufaginol R=OH, R1=H, R2=H, R3=CH2OH
23 resibufogenin R=OH, R1=H, R2=H, R3=CH3
24 3α-hydroxy-regibufogenin R=H, R1=OH, R2=H, R3=CH3
25 resibufogenin-3-acetate R=OCOCH3, R1=H, R2=H, R3=CH3
26 3-oxo-resibufogenin R+R1=O, R2=H, R3=CH3
27 Δ^1-3-oxo-resibufogenin R+R1=O, R2=H, R3=CH3, Δ1
28 $\Delta^{1,4}$-3-oxo-resibufogenin R+R1=O, R2=H, R3=CH3, Δ1,4
29 16α-hydroxy-resibufogenin-3-acetate R=OCOCH3, R1=H, R2=H, R3=CH3, 16α-OH
30 14α,15α-epoxy-resibufogenin R=OH, R1=H, R2=H, R3=CH3, 14α,15α-epoxy
31 3α-hydroxy-14α,15α-epoxy-resibufogenin R=H, R1=OH, R2=H, R3=CH3, 14α,15α-epoxy
32 3-oxo-14α,15α-epoxy-resibufogenin R+R1=O, R2=H, R3=CH3, 14α,15α-epoxy
33 14α,15α-epoxy-resibufogenin-3-acetate R=OCOCH3, R1=H, R2=H, R3=CH3, 14α,15α-epoxy
34 14α,15α-epoxy-resibufogenin-3α-acetate R=H, R1=α-OCOCH3, R2=H, R3=CH3, 14α,15α-epoxy
35 marinobufagin R=OH, R1=H, R2=OH, R3=CH3

Figure 1. Structures of bufadienolides (**1–62**), cardenolides (**63–68**) and α-pyrone opening compounds (**69–80**).

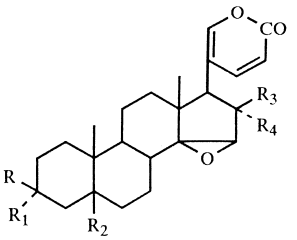

Group B

36 cinobufagin R=OH, R1=H, R2=H, R3=$OCOCH_3$, R4=H
37 3α-hydroxy-cinobufagin R=H, R1=OH, R2=H, R3=$OCOCH_3$, R4=H
38 cinobufagin-3-acetate R=$OCOCH_3$, R1=H, R2=H, R3=$OCOCH_3$, R4=H
39 cinobufagin-3-succinate R=$OCO(CH_2)_2COOH$, R1=H, R2=H, R3=$OCOCH_3$, R4=H
40 cinobufagin-3-suberate R=$OCO(CH_2)_6COOH$, R1=H, R2=H, R3=$OCOCH_3$, R4=H
41 cinobufagin-3-cinnamate R=$OCOCH{=}CHC_6H_5$, R1=H, R2=H, R3=$OCOCH_3$, R4=H
42 3-oxo-cinobufagin R+R1=O, R2=H, R3=$OCOCH_3$, R4=H
43 cinobufagin-3,5-dinitrobenzoate R=$OCO[3,5\text{-}(NO_2)_2C_6H_3]$, R1=H, R2=H, R3=$OCOCH_3$, R4=H
44 3,16-diketo-cinobufagin R+R1=O, R2=H, R3+R4=O
45 16-oxo-cinobufagin-3-acetate R=$OCOCH_3$, R1=H, R2=H, R3+R4=O
46 desacetyl-cinobufagin R=OH, R1=H, R2=H, R3=OH, R4=H
47 desacetyl-cinobufagin-3-acetate R=$OCOCH_3$, R1=H, R2=H, R3=OH, R4=H
48 desacetyl-cinobufagin-3-acetate-16-succinate R=$OCOCH_3$, R1=H, R2=H, R3=$OCO(CH_2)_2COOH$, R4=H
49 desacetyl-14α,15α-epoxy-cinobufagin-3-acetate R=$OCOCH_3$, R1=H, R2=H, R3=OH, R4=H, 14α,15α-epoxy
50 cinobufotalin R=OH, R1=H, R2=OH, R3=$OCOCH_3$, R4=H
51 desacetyl-cinobufotalin R=OH, R1=H, R2=OH, R3=OH, R4=H

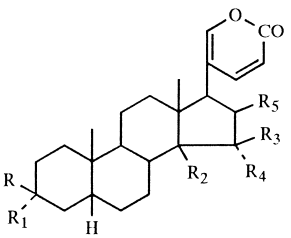

Group D

52 β-chlorohydrin R=OH, R1=H, R2=Cl, R3=H, R4=OH, R5=H
53 14β-artebufogenin R=OH, R1=H, R2=H, R3+R4=O, R5=H
54 14β-artebufogenin-3-acetate R=$OCOCH_3$, R1=H, R2=H, R3+R4=O, R5=H
55 14α-artebufogenin R=OH, R1=H, R2=α–H, R3+R4=O, R5=H
56 3-oxo-14α-artebufogenin R+R1=O, R2=α–H, R3+R4=O, R5=H
57 Δ^{14}-bufalin R=OH, R1=H, R2+R3+R4=Δ, R5=H
58 Δ^{14}-3-oxo-bufalin R+R1=O, R2+R3+R4=Δ, R5=H
59 Δ^{14}-bufotalin-3-acetate R=$OCOCH_3$, R1=H, R2+R3+R4=Δ, R5=$OCOCH_3$

Group A

60 15α-hydroxy-bufalin R=OH, R1=H, R2=OH, R3=H, R4=OH, R5=H
61 15α-hydroxy-bufalin-3-acetate R=$OCOCH_3$, R1=H, R2=OH, R3=H, R4=OH, R5=H
62 15-oxo-bufalin-3-acetate R=$OCOCH_3$, R1=H, R2=OH, R3+R4=O, R5=H

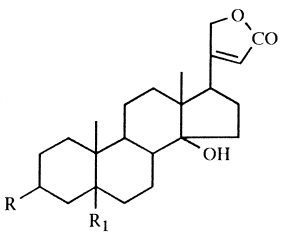

Group C

63 periplogenin R=OH, R1=OH
64 digitoxigenin R=OH, R1=H
65 digitoxigenin-3-acetate R=$OCOCH_3$, R1=H
66 digitoxigenin-3-suberate R=$OCO(CH_2)_6COOH$, R1=H
67 digitoxigenin-3-methylsuberate R=$OCO(CH_2)_6COOCH_3$, R1=H
68 Δ^{14}-digitoxigenin R=OH, R1=H, Δ14

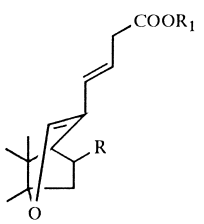

Group E

69 isobufalin R=H, R1=H
70 isobufalin Me-ester R=H, R1=CH_3
71 isobufalin Me-ester-3-acetate R=H, R1=CH_3, 3-$OCOCH_3$
72 isobufalin Et-ester R=H, R1=C_2H_5
73 isobufalin Et-ester-3-acetate R=H, R1=C_2H_5, 3-$OCOCH_3$
74 isobufotalin Me-ester-3-acetate R=$OCOCH_3$, R1=CH_3, 3-$OCOCH_3$
75 isogamabufotalin-Me-ester-3,11-diacetate R=H, R1=CH_3, 3-$OCOCH_3$, 11α-$OCOCH_3$

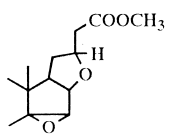

76 CMKA

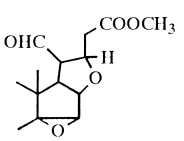

77 CMKB

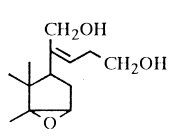

78 RRA-1

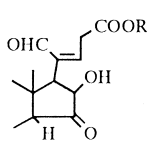

79 14β-arte-MK R=CH_3
80 14β-arte-Et-K-Ac R=C_2H_5, 3-$OCOCH_3$

Figure 1.—*contd.*

showed lower activity than that of other compounds having oxygen group at C-14, it was suggested that oxygen at C-14 position had more important effect than the steroidal structure on the activity. On the other hand, the activity of 10^{-2} order of β-chlorohydrin (**52**) having 14β-Cl group was slightly higher than that of resibufogenin (**23**) having 14β, 15β-epoxy group. Also, the IC_{50} value of 14β-artebufogenin (**53**) (14β-H) was stronger than that of corresponding 14α-H isomer (**55**). This demonstrated that the compounds having *cis* C/D ring junction had higher cytotoxicities than those with *trans* junction.

Group E (69–80)

Those compounds having each opened α-pyrone ring moiety (**69**–**80**) had more or less the same effect on the cells, suggesting that α-pyrone ring was apparently not a necessary requirement for the cytotoxicities on PLC cells of bufadienolides.

In an over view, the biological evaluation of 14-hydroxy and 14, 15-epoxy as well as 14-artebufogenins revealed that the configuration is crucial for the cytotoxicity: those having β type configuration is superior to those having α configuration. Deoxygenation at C-14 reduced the activity. The 14β-hydroxy derivatives having 16-acetoxy group reduced activity, whereas the 14β, 15β-epoxy derivatives increased it. The activity of 3β-ester and 3-ketone derivatives were reduced, comparing with those of the corresponding parent compounds. The activity was increased when 3β-hydroxy substituents were converted to 3β-acetate in the 14β-hydroxy derivatives, but decreased in the 14β, 15β-epoxy derivatives. It is distinctly possible that a combination of various substituents at C3, C19, and D ring may occur potency of inhibition in cell growth. The important structural features which influence the cytotoxic activities of naturally occurring bufadienolide, cardenolide, and their derivatives were summarized in Figure 2. Thus, 17-α-pyrone ring, 3β, 14β-hydroxyls, and the ring junction (C/D *cis*) in bufadienolides were apparently most crucial requirement for the potent cytotoxic activity.

DISCO analysis

For preparation of pharmacophore model, 2D structures was converted into the 3D structures to translate the 2D structure–activity information into the 3D requirements for the activity. In the present study, 16 bufadienolides, showing potent cytotoxic activities ($IC_{50} < 10^{-3}$), were chosen as active compounds. For each of the preferred conformations the points to be considered in the superposition step were chosen and their locations were determined by calculation. These points included not only the atoms in the molecule but also the central points of aromatic ring centroids, and the points locating between the hydrogen-bond donors and acceptors in hydrogen bondings. The points of hydrogen bonds involved in this calculation were carbonyl

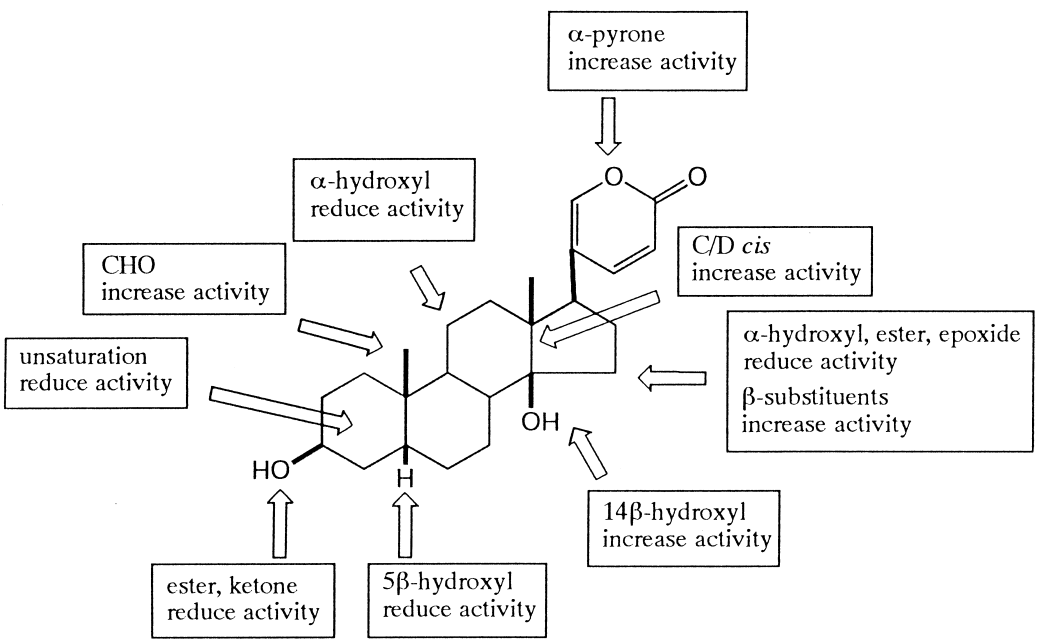

Figure 2. Effects of various partial structures and groups on cytotoxic activities of naturally occurring bufadienolides, cardenolides and their related analogues. The structure is a bufalin.

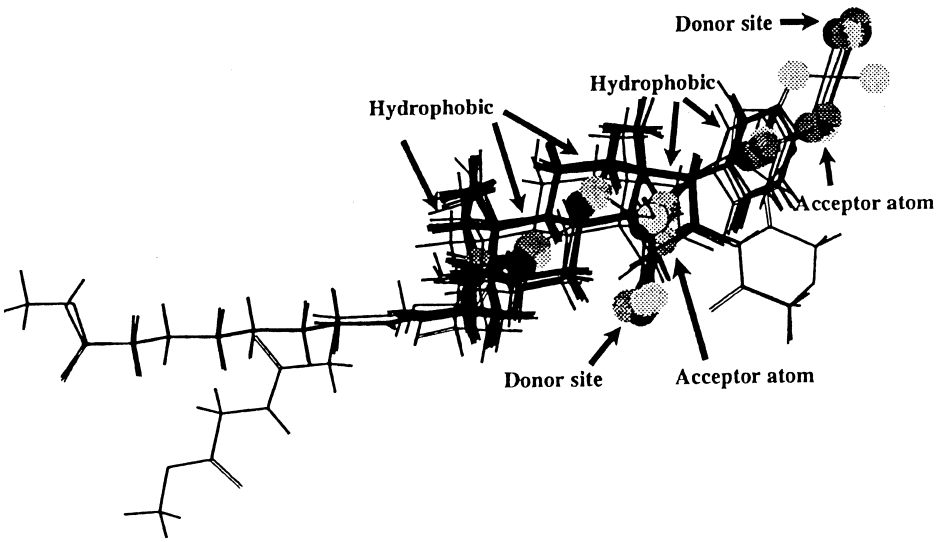

Figure 3. Superimposed structures of 16 bufadienolides analysed by DISCO.

oxygens normally interacted with hydrogen-bond donors in the directions of an angle of 120°, having the distance of 2.9–3.0 Å between the carbonyl oxygen and the hydrogen. On the basis of these chemical similarities such as hydrophobic, hydrogen-bond donating or accepting groups, the preferred conformers were examined for their superimposability by the program DISCO.[3]

In the present survey, for the least squares fitting, three points, i.e. the hydrophobic ring centroid of steroidal backbone, and the points locating between the donor and acceptor atoms of hydrogen bonds, involving the two electron lone pairs of the oxygen atoms, of bufalin 3-acetate (**3**) as a template molecule were chosen. DISCO is usually instructed to iterate the tolerance at which two inter-point distances are considered the same. The maximum tolerance of these features, i.e. hydrophobic ×5, acceptor atom ×2, and donor site ×2 shown in Figure 3, of the 16 bufadienolides was 1.5 Å indicating that the three dimensioned structures including these features was well superimposed (Figure 3). The mean of the distances among these features was 5.94 Å.

Table 2. Summary of CoMFA-PLS results (PLC cells)

No. of compounds	70
Opt. no. of components	5
Prob atom	c (sp^3, +1)
Cross-validated r^2	0.326
Std error of estimate	0.729
r^2	0.803
F values	52.297
Contributions	
Steric	0.468
Electrostatic	0.532

CoMFA analysis

The above SAR studies indicated that a combination of various substituents may increase the cell growth inhibition. In applying these results in QSAR studies, one of the important goals is the quantitative correlation

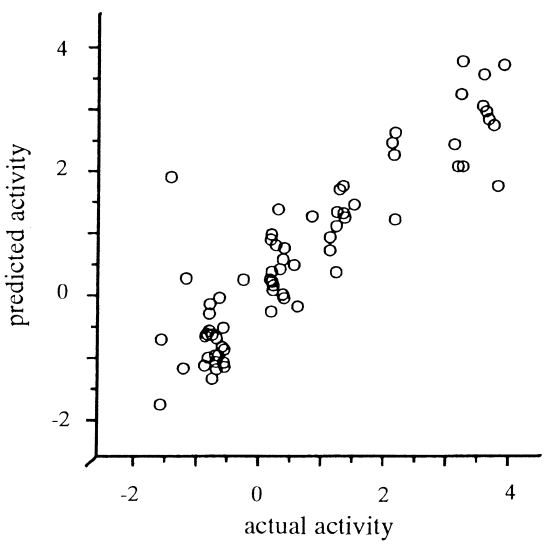

Figure 4. Plot of actual vs predicted inhibitory activities on cells of primary liver carcinoma PLC/PRF/5 ($r^2 = 0.803$). The activities are expressed by log $1/IC_{50}$.

between 3D molecular structure and biological function, which is subsequently predictable of this property for novel compounds.

Analysis was performed for 70 kinds of natural and semisynthetic analogues, which excluded 10 analogues synthesized in this study. First, 'leave-one-out' cross-validation was used so that each compound would be systematically excluded and its activity predicted by the analysis during formulation of the regression equation. For this set, acceptable q2 (0.326) was obtained. Second PLS analysis was performed by using the optimum number of components with no cross-validation. The results of a non-cross-validated PLS analysis using the 70 compounds are listed in Table 2, and the actual, predicted activity and residuals are shown in Table 3. It is evident that the CoMFA-derived QSAR manifested a relatively good cross-validated r^2 and indicating thereby a considerable predictive and correlative capacity for growth inhibition of the PLC cells, regardless of its large number of samples ($n=70$). The relative contributions of the steric and electrostatic fields to this model were almost equal. Evidence for the predictive performance of the CoMFA-derived model is provided in Figure 4 which shows plots of actual versus predicted growth inhibitions [log $(1/IC_{50})$].

The major steric and electrostatic features of the QSAR are represented in Figure 5 in the form of three-dimensional contour maps, displayed as transparent surfaces. The surfaces at the top in Figure 5 indicate the areas in space around the template molecule (**19**) where increases

Table 3. Actual, predicted activities and residuals from CoMFA analysis

	log $1/IC_{50}$ (PLC)						
Compds	Actual	Predicted	Residual	Compds	Actual	Predicted	Residual
1	3.55	2.74	0.81	**41**	−0.81	−0.78	−0.03
2	1.12	1.25	−0.13	**42**	1.25	1.15	0.10
3	3.70	1.67	2.03	**43**	0.11	0.07	0.04
6	3.12	3.68	−0.56	**44**	0.07	−0.35	0.43
7	2.05	2.54	−0.49	**45**	−0.38	0.16	−0.54
9	2.03	2.17	−0.14	**46**	0.28	−0.13	0.42
10	−0.88	−0.72	−0.16	**47**	1.01	0.63	0.38
11	3.51	2.88	0.63	**49**	0.06	0.16	−0.11
12	0.72	1.18	−0.46	**50**	3.00	2.34	0.66
13	3.47	3.47	0.00	**51**	0.17	1.28	−1.11
14	3.11	3.15	−0.04	**52**	1.15	1.61	−0.46
15	3.64	2.65	0.99	**53**	0.09	0.13	−0.04
16	1.22	1.23	−0.01	**54**	0.26	−0.07	0.33
17	0.10	−0.01	0.11	**55**	−0.91	−0.23	−0.68
18	3.46	2.96	0.50	**57**	0.08	0.28	−0.20
19	3.80	3.62	0.17	**58**	−0.69	−1.17	0.48
20	0.06	0.80	−0.74	**59**	−0.70	−0.61	−0.09
21	2.05	1.12	0.93	**60**	−1.54	1.81	−3.35
22	0.22	0.33	−0.11	**61**	0.15	0.71	−0.56
23	1.11	0.27	0.84	**62**	1.11	1.02	0.09
24	−0.92	−0.38	−0.54	**63**	1.22	1.67	−0.45
25	0.50	−0.27	0.76	**64**	3.06	1.98	1.08
26	−0.76	−0.13	−0.63	**65**	0.26	0.48	−0.22
29	−0.83	−1.05	0.22	**66**	−0.72	−0.91	0.20
30	−1.30	0.18	−1.48	**68**	0.44	0.39	0.06
31	−0.67	−1.24	0.56	**69**	−1.00	−1.22	0.22
32	−0.94	−1.09	0.15	**70**	−0.96	−0.72	−0.24
33	−0.77	−1.06	0.29	**71**	−0.82	−1.16	0.34
34	−0.67	−0.95	0.28	**72**	−0.88	−1.44	0.56
35	0.28	0.67	−0.39	**73**	−0.81	−1.27	0.47
36	3.13	1.99	1.15	**74**	−1.69	−0.80	−0.89
37	1.01	0.84	0.17	**75**	−0.99	−0.75	−0.24
38	1.40	1.37	0.03	**78**	−1.70	−1.84	0.14
39	0.07	0.88	−0.81	**79**	−0.92	−0.66	−0.27
40	2.00	2.37	−0.37	**80**	−1.34	−1.27	−0.08

(green region) and/or decreases (yellow region) in steric bulk could enhance growth inhibition of PLC cells. Contour maps of the electrostatic field contributions are also provided in Figure 5.

The steric field map indicated that presence of steric bulk of a type configuration at C-14 and -15 has a measurable negative effect on the activity, as mentioned in the SAR consideration as discussed above. Less bulk favorable regions are indicated around the α-pyrone ring and the side chain at C-3 lowers the cytotoxicity. On the other hand, more bulky side chain at C-14 and -15 of β configuration enhances the activity, suggesting that β type configuration favors the activity more than that of α type for the C-14 and/or -15 substituents of the compounds.

In the electrostatic CoMFA map, the region where a more positive electrostatic interaction might be expected to enhance the growth inhibition activity, was encompassed

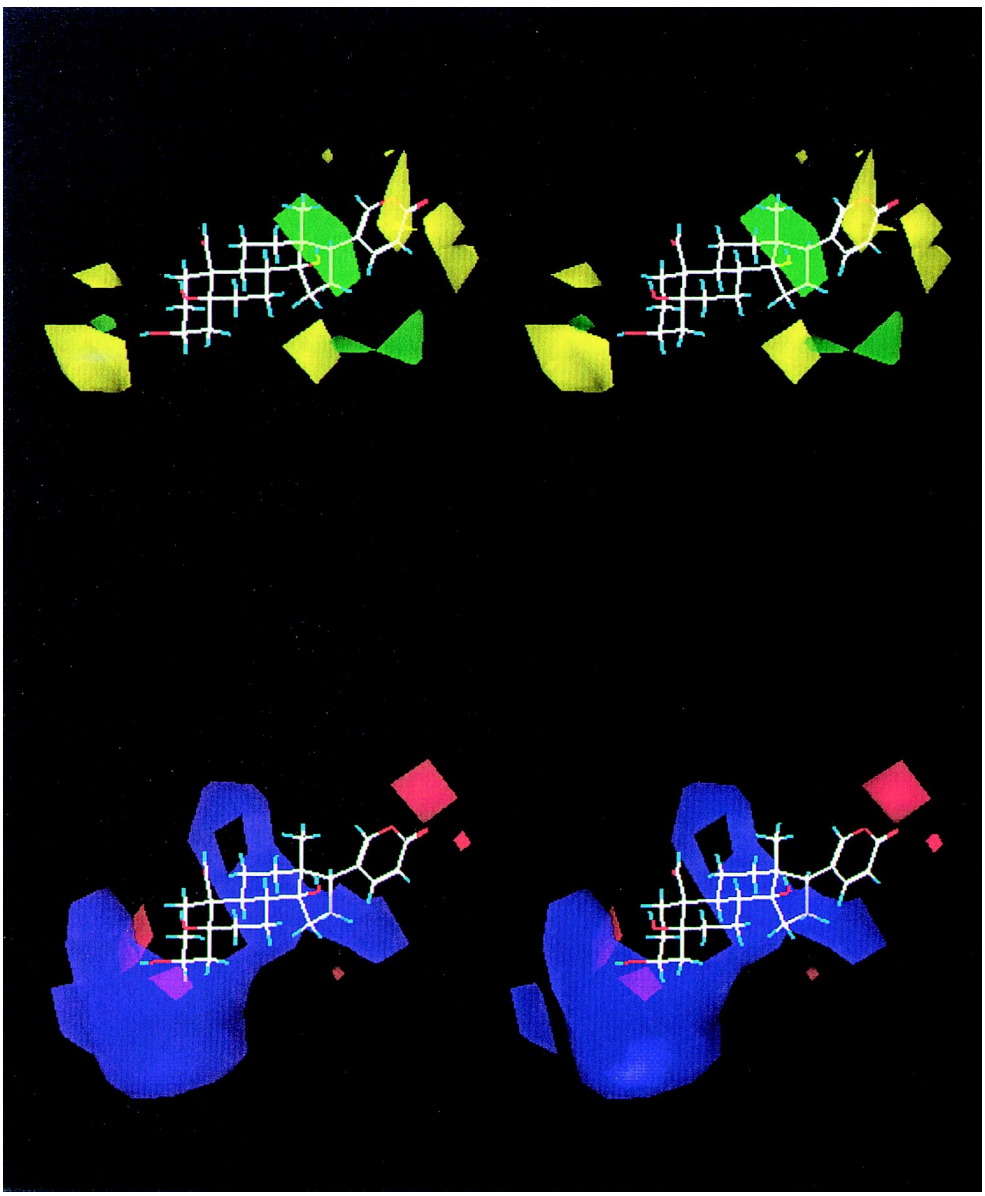

Figure 5. Stereoviews of CoMFA contour plots from the PLS analysis. Above: steric, below: electrostatic. Regions where increased steric bulk is associated with enhanced activity are indicated in green, whereas regions where increased steric bulk is associated with diminished activity are indicated in yellow. On the other hand, regions where increased positive charge is favorable for activity are indicated in blue, whereas regions where increased negative charge is favorable are indicated in red.

around the α-face around the steroidal backbone skeleton. The regions of negative electrostatic interactions were scattered around the ester side chains at C-3 and -5, and the α-pyrone ring.

The CoMFA model derived from the above bufadienolides was used to estimate the IC_{50} values of the test bufadienolides, we synthesized in this study. The observed and corresponding CoMFA-predicted IC_{50} values for the test-set bufadienolides are as follows (observed: predicted): bufalin 3-succinate (**4**): (1.18:1.41), bufalin 3-methacrylate (**5**) (1.20:0.94), bufalin 3-[*N*-(*tert*-butoxycarbonyl) hydrazido] succinate (**8**) (1.12:0.94), Δ^1-3-oxo-resibufogenin (**27**) (1.12:0.94), $\Delta^{1,4}$-3-oxo-resibufogenin (**28**) (0.35:0.84), desacetyl-cinobufagin 3-acetate-16-succinate (**48**) (1.12:0.94), 3-oxo-14α-artebufogenin (**56**) (1.12:0.94), digitoxigenin 3-methylsuberate (**67**) (1.12:0.94), CMKA (**76**) (1.12:0.94), and CMKB (**77**) (1.12:0.94). These comparison shows that this model can generally predict the activity of the active derivatives, though it may need to test for inactive derivatives.

In summary, we established 3D-QSAR models by using the CoMFA methodology for a set of 70 bufadienolides that are known to inhibit the growth of primary liver carcinoma PLC/PRF/5 cells in vitro. To identify a common pharmacophore and to elucidate a common binding model, DISCO was used to systematically compare low-energy conformations of the analogues. The results provided a correlation between the inhibitory activity of these bufadienolides and the steric and electrostatic fields around them. The QSAR models reveal regions in three dimensional space around these analogues. The models obtained in this study are reasonably predictive, as indicated by the cross-validated r^2 values, and also provided predictions which agreed well with experimental values. This model should be useful for the new drug designing of this series which possess higher affinity and selectivity.

References

1. Yoshida, S.; Kamano, Y.; Sakai, T. *Chem. Pharm. Bull.*, **1976**, *24*, 1714–1717.

2. Jing, Y.; Ohizumi, H.; Kawazoe, N. et al., *Jpn. J. Cancer Res.*, **1994**, 85/645.

3. Martin, Y. C.; Bures, M. G.; Danaher, E. A.; DeLazzer, J.; Lico, I.; Pavlik, P. A., *J. Computer-Aided Mol. Design*, **1993**, *7*, 83.

4. Cramer, R. D.; Patterson, D. E.; Bunce, J. D. *J. Am. Chem. Soc.*, **1988**, *110*, 5959–5967.

5. Kamano, Y.; *Kagaku No Rhoiki*, **1970**, *24*, 339–354 and 421–432.

6. Kamano, Y.; Pettit, G. R.; Inoue, M.; Tozawa, M.; Komeichi, Y. *J. Chem. Research(S)*, **1977**, 78–79, and *J. Chem. Research(M)*, **1977**, 0843–0859.

7. Pettit, G. R.; Kamano, Y.; Inoue, M.; Komeichi, Y.; Nassimbeni, L. R.; Niven, M. L. *J. Org. Chem.*, **1982**, *47*, 1503–1505.

8. Kamano, Y.; Yamamoto, H.; Tanaka, Y.; Komatsu, M. *Tetrahedron Lett.*, **1986**, *54*, 5673–5676.

9. Kamano, Y.; Satoh, N.; Nakayoshi, H.; Pettit, G. R.; Smith, C. R. *Chem. Parm. Bull.*, **1988**, *36*, 326–332.

10. Kamano, Y.; Pettit, G. R. *J. Am. Chem, Soc.*, **1972**, *94*, 8592.

11. Kamano, Y.; Pettit, G. R. *J. Org. Chem.*, **1974**, *39*, 2629–2631.

12. Pettit, G. R.; Kamano, Y. *J. Chem., Soc., Perkin Trans. I*, **1973**, 725–727.

13. a) Hofer, P.; Linde, H.; Meyer, K. *Tetrahedron Lett.*, **1959**, 8. b) Hofer, P.; Linde, H.; Meyer, K. *Helv. Chim. Acta.*, **1960**, *43*, 1950.

14. Kamano, Y.; Yamamoto, H.; Hatayama, K.; Tanaka, Y.; Shinihara, M.; Komatsu, M. *Tetrahedron Lett.*, **1968**, *54*, 5669–5672.

15. Kamano, Y.; Hatayama, K.; Shinohara, M; Komatsu, M. *Chem. Pharm. Bull.*, **1971**, *19*(12), 2478–2484.

16. Kamano, Y.; Kumon, S.; Arai, T.; Komatsu, M. *Chem. Pharm. Bull.*, **1973**, *21*(9), 1960–1964.

17. Kamano, Y.; Pettit, G. R.; Inoue, M.; Tozawa, M.; Smith, C. R.; Weislder, D. *J. Chem., Soc., Perkin Trans*, **1988**, 2037–2041.

18. Kamano, Y. *Chem. Pharm. Bull.*, **1969**, *17*(8), 1711–1719.

19. Pettit, G. R.; Kamano, Y. *J. Org. Chem.*, **1972**, *37*, 4040–4044.

20. Kamano, Y.; Dralsar. P.; Pettit, G. R.; Tozawa, M. *Collection Czechoslovak Chem. Commum.*, **1987**, *52*, 1325–1330.

21. Kamano, Y.; Pettit, G. R. *Chem. Pharm. Bull.*, **1973**, *21*(4), 895–898.

22. Horiger, N.; Zivanov, D.; Linde, H.H.A.; Meyer, K. *Helv. Chim. Acta*, **1970**, *53*, 1993.

23. Kamano, Y.; Pettit, G. R.; Brown P.; Inoue, M. *Tetrahedron*, **1975**, *31*, 2359–2361.

24. Kamano, Y.; Pettit, G. R.; Tozawa, M.; Komeichi, Y.; Inoue, M. *J. Org. Chem.*, **1975**, *40*, 2136–2138.

25. Kamano, Y.; Pettit, G. R. *J. Chem. Soc., Perkin Trans*, **1975**, 1976–1978.

26. Kamano, Y.; Tozawa, M.; Pettit, G. R. *J. Org. Chem.*, **1975**, *40*, 793–795.

27. Kamano, Y.; Komatsu, M. *Chem. Pharm. Bull.*, **1969**, *17*(8), 1698–1705.

28. Kamano, Y.; Yamamoto, H.; Komatsu, M. *Chem. Pharm. Bull.*, **1969**, *17*(6), 1246–1250.

29. Kamano, Y.; Tanaka, Y.; Komatsu, M. *Chem. Pharm. Bull.*, **1969**, *17*(8), 1706–1710.

30. Gasteiger, J.; Marsili, M. *Tetrahedron*, **1980**, *36*, 3219–3228.

31. Stahle, L.; Wold, S. *Progr. Med. Chem.*, **1988**, *25*, 292–334.